PERFORMANCE ANALYSIS OF MULTIANTENNA WIMAX SYSTEMS OVER FREQUENCY-SELECTIVE FADING CHANNELS

D. Molteni[(1)], M. Nicoli[(1)], R. Bosisio[(1)], L. Sampietro[(2)]
[(1)]Dipartimento di Elettronica e Informazione, Politecnico di Milano, Piazza L. da Vinci 32, I-20133 Milano, Italy
[(2)]Nokia Siemens Networks S.p.A., S.S. 11 km 158, 20060 Cassina de' Pecchi (Milano), Italy
e-mail: {nicoli,rbosisio}@elet.polimi.it, Luigi.Sampietro@siemens.com

Abstract

A multicell WiMax system which supports orthogonal frequency division multiplexing (OFDM) and antenna arrays at the base stations is considered in this paper as conforming to the IEEE 802.16-2004 standard. Focusing on the uplink, we propose an analytical framework to assess the average error probability of the system over time-dispersive (or, equivalently, frequency selective) and space-dispersive (due to the antenna array) Rayleigh fading channels. The proposed method takes into account the effects of the correlation of the channel gains over the space-frequency domain, the power-angle structure of the inter-cell interference, the array processing at the base station and the interleaving scheme. Simulation results corroborate the proposed analysis for a IEEE 802.16-2004 cellular system over different propagation scenarios.

I. Introduction

Worldwide Interoperability for Microwave Access (WiMax) is a standard based technology that provides last mile broadband wireless access. In this paper, we consider multicell WiMax systems conforming to the IEEE 802.16-2004 standard [1] [2], which prescribes the employment of OFDM modulation and supports antenna array technology. The pushing demand for broadband systems makes WiMax one of the most promising technologies for the near future in wireless communications. The system is expected to operate in heterogeneous propagation environments as applications range from the provisioning of wireless services in rural areas to intensive and real-time applications on notebooks and other mobile devices. Thereby, a thorough analysis of its performance under realistic and different propagation environments is mandatory.

Several works have recently focused on the evaluation of the error rate of bit-interleaved coded OFDM systems over frequency selective fading channels [3]-[5]. To simplify the performance evaluation, the concept of *effective signal-to-noise ratio* (SNR) has been introduced in [3] as the SNR of an equivalent additive white Gaussian noise (AWGN) channel which would yield the same error probability as that of the considered frequency-selective channel. The effective SNR can be used to adapt modulation and coding to the instantaneous channel conditions (and the service requirements) or to assess the average error rate for a given transmission mode [4]. Average and outage system performances have also been derived in [5] for multiantenna combining techniques in Nakagami-fading propagation environments, while the effects of non-stationary intercell interference on the performance of multiantenna WiMax systems have been studied in [6] [7].

In this paper we develop a unified framework to analytically assess the uplink performance of a multiantenna WiMax system over *space-time* dispersive Rayleigh-fading environments with *spatially correlated* intercell interference. The array processing at the base station is here optimized for the mitigation of out-of-cell interference impairments. Different angle-delay spreads are investigated by introducing an efficient description of the long-term features of the multipath channel which allows to simplify the parametrization of the space-frequency channel correlation. For each channel model, the code error rate is expressed as a function of the effective signal to interference plus noise ratio (SINR), here re-defined with respect to the single-antenna analysis [4] so as to *jointly* account for the correlation of the inter-cell interference over the antennas and the correlation of the channel gains over *both* the antennas *and* the subcarriers. The performance analysis is carried out so as to fit the specific WiMax standard and to account for the effects of the standard-compliant interleaving scheme. A closed-form expression of the distribution of the effective SINR is derived, for each Hamming distance of the convolutional code (CC), through an eigenvalue decomposition of the space-frequency channel covariance matrix. Finally, the average bit-error-rate (BER) is obtained by the conventional truncated union bound [8]. Numerical results show that the proposed analytical model provides an accurate fitting of the BER over a large range of space-time multipath environments.

II. System description

A. Multi-cell layout

We consider the uplink of a IEEE 802.16-2004 multicell system [1] [2] with fixed subscriber stations (SS). Base stations (BS) are distributed over the access area as indicated in Fig. 1, forming an hexagonal cellular layout with frequency reuse factor 3. In this example, the transmission by the subscriber station SS_0 to its own base station BS_0 is impaired by the interference from $N_I = 3$ out-of-cell subscriber stations $\{SS_i\}_{i=1}^{N_I}$ which transmit using the same time-slot and the same frequency band as SS_0; BS_0 is equipped with a uniform linear array (ULA) of M antennas covering a 120deg sector, while SSs have a single antenna.

B. System model

According to the standard, a sequence of bits $\{b_k\}$ is convolutionally coded at the transmitter, bit-interleaved and mapped into complex symbols $\{x_k\}$ belonging to the constellation of the selected digital modulation. For the sake of simplicity, here we restrict the analysis to the first of the seven modulation-coding schemes of the standard [1] [2], employing BPSK

1-4244-1144-0/07/$25.00

modulation and a CC encoder with rate 1/2 and generators (171,133). Though the standard prescribes also an outer Reed Solomon code, for the BPSK mode the outer code is disabled.

The modulated symbols are transmitted by OFDM signalling over a frequency selective fading channel and received by the base station BS_0 in AWGN and inter-cell interference. OFDM demodulation is carried out at each receiving antenna, so that the $M \times 1$ baseband signal obtained at the output of the M demodulators on the kth subcarrier can be written as

$$\mathbf{y}_k = \mathbf{h}_k x_k + \mathbf{n}_k, \quad (1)$$

where the $M \times 1$ vector $\mathbf{h}_k$ gathers the M (complex) channel gains between the transmitter SS_0 and the M antennas at BS_0, while x_k denotes the symbol transmitted by SS_0. The vector $\mathbf{n}_k$ models the background noise and the inter-cell interference generated by the users $\{SS_i\}_{i=1}^{N_I}$. It is assumed to be zero-mean Gaussian, temporally uncorrelated but spatially correlated (due to the interference) with spatial covariance matrix $\mathbf{Q} = \mathrm{E}[\mathbf{n}_k \mathbf{n}_k^{\mathrm{H}}] = \sigma_n^2 \mathbf{I}_M + \mathbf{Q}_I$, where σ_n^2 is the variance of the background noise while $\mathbf{Q}_I$ denotes the contribution from the N_I active interferers. The subcarrier index, $k \in \mathcal{K} = \{k_1, \ldots, k_K\}$, ranges over the K subcarriers used for data transmission. The total number of subcarriers is $N = K + P + G + 1$, which includes also the pilots (P), the guard-band subcarriers (G) and the DC. We further assume that the length of each codeword equals the OFDM symbol length K. The other main system parameters are listed in Table 1.

To reduce the interference effects, BS_0 applies the minimum variance distortionless (MVDR) filter [10] to the signal (1):

$$\hat{x}_k = (\mathbf{h}_k^{\mathrm{H}} \mathbf{Q}^{-1} \mathbf{h}_k)^{-1} \mathbf{Q}^{-1} \mathbf{h}_k^{\mathrm{H}} \mathbf{y}_k = x_k + (\tilde{\mathbf{h}}_k^{\mathrm{H}} \tilde{\mathbf{h}}_k)^{-1} \tilde{\mathbf{h}}_k^{\mathrm{H}} \tilde{\mathbf{n}}_k. \quad (2)$$

To simplify the notation, $\tilde{\mathbf{h}}_k = \mathbf{Q}^{-\mathrm{H}/2} \mathbf{h}_k = [\tilde{h}_{k,1} \cdots \tilde{h}_{k,M}]^{\mathrm{T}}$ has been introduced to denote the channel vector weighted by the Hermitian Cholesky factor of the noise spatial covariance $\mathbf{Q}$, while $\tilde{\mathbf{n}}_k = \mathbf{Q}^{-\mathrm{H}/2} \mathbf{n}_k$ is the whitened noise vector. It can be easily shown that the signal-to-interference-plus-noise ratio (SINR) at the output of the spatial filter is [10]:

$$\gamma_k = \frac{\mathrm{E}\left[|x_k|^2\right]}{\mathrm{E}\left[|\hat{x}_k - x_k|^2\right]} = \sum_{m=1}^{M} |\tilde{h}_{k,m}|^2 = ||\tilde{\mathbf{h}}_k||^2. \quad (3)$$

The output symbols $\hat{x}_k$ are then used for soft demodulation, bit deinterleaving, bit maximum-a-posteriori (MAP) convolutional decoding.

C. Channel and interference model

Let $\mathbf{H}$ be the $M \times K$ space-frequency matrix that gathers the channel gains for the M antennas and the K subcarriers over the link SS_0-BS_0:

$$\mathbf{H} = [\mathbf{h}_1 \cdots \mathbf{h}_K] = \sqrt{P_0} \sum_{r=1}^{N_R} \alpha_r \mathbf{a}(\theta_r) \mathbf{g}^{\mathrm{T}}(\tau_r). \quad (4)$$

This matrix is here modelled as the sum of N_R path contributions, each characterized by a direction of arrival (DOA)

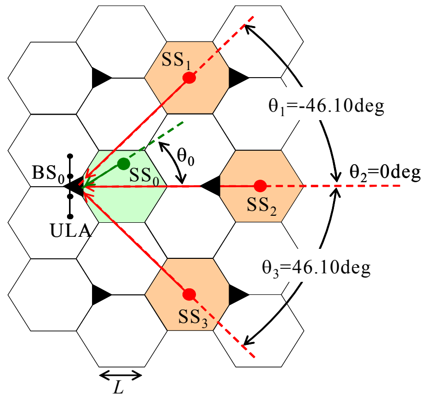

Figure 1: Cellular layout with hexagonal cells: shaded cells represent the first ring of interference for reception of the user SS_0 by the base station BS_0.

θ_r, a time of arrival (TOA) τ_r and a complex fading amplitude α_r. The average power received from all paths is indicated by P_0, while the $M \times 1$ vector $\mathbf{a}(\theta_r) = [a_1(\theta_r) \cdots a_M(\theta_r)]^{\mathrm{T}}$ represents the ULA response to the DOA θ_r. The $K \times 1$ vector $\mathbf{g}(\tau_r) = [g_1(\tau_r) \cdots g_K(\tau_r)]^{\mathrm{T}}$ contains the K samples of the N-point discrete Fourier transform (DFT) of the channel impulse response over the rth path, i.e.:

$$g_i(\tau_r) = G_{k_i} \exp\left(-j2\pi \frac{k_i}{N} \frac{\tau_r}{T}\right) \text{ for } i = 1, \ldots, K, \quad (5)$$

where G_{k_i} is the frequency response of the cascade connection of the transmitter and receiver filters on the k_ith subcarrier (for $k_i \in \mathcal{K}$). To simplify, TOAs are simulated as integer multiple of the sampling interval T, so that $\forall k_i$, $G_{k_i} = 1$. Amplitudes are assumed to be uncorrelated Rayleigh-faded, $\alpha_r \sim \mathcal{CN}(0, \rho(\tau_r, \theta_r))$, with variance $\rho(\tau_r, \theta_r)$ that depends on the power-delay-angle profile (PDAP) $\rho(\tau, \theta)$. The PDAP is here modelled as $\rho(\tau, \theta) = \rho_{\mathrm{d}}(\tau)\rho_{\mathrm{a}}(\theta, \theta_0)$, with exponential profile $\rho_{\mathrm{d}}(\tau)$ over the delays and Laplacian (double exponen-

Table 1: Relevant system parameters.

Carrier frequency f_c	3.5GHz
Sampling frequency $1/T$	4MHz
N. of subcarriers N	256
N. of guard-band subcarriers G	$28 + 27$
N. of pilots P	8
N. of data subcarriers K	192
Maximum cyclic prefix length N_{cp}	64 samples
N. of antennas M	4
Antenna spacing Δ	1.4λ
Path loss exponent υ	3
CC generators (rate 1/2)	(171,133)
CC minimum Hamming distances	10,12

tial) profile $\rho_{\rm a}(\theta, \theta_0)$ over the angles:

$$\rho_{\rm d}(\tau) = \rho_{\rm d}(0) \exp\left(-\frac{\tau}{\sigma_\tau}\right) \; \tau \geq 0, \quad (6)$$

$$\rho_{\rm a}(\theta, \theta_0) = \rho_{\rm a}(0, \theta_0) \exp\left(-\frac{|\theta - \theta_0|}{\sigma_\theta}\right). \quad (7)$$

The angle θ_0 denotes the main DOA connecting SS_0 and BS_0, while the scalar terms $\rho_{\rm d}(0)$ and $\rho_{\rm a}(0, \theta_0)$ are used to normalize each power profile to one, so that $\sum_{r=1}^{N_R} \rho(\tau_r, \theta_r) = 1$. The decaying constants σ_τ and σ_θ will be referred to as, respectively, delay and angle spread of the channel.

As further performance references, we consider also two simplified Rayleigh-fading models that can be seen as extreme cases of frequency selectivity:

- Frequency-flat channel (FF): the channel gains are constant over the subcarriers (as for a null delay spread, i.e. $\tau_r = 0, \forall r$);
- Maximum frequency diversity (FD): the channel gains are independent identically distributed over the subcarriers (as for the ideal case of a maximum delay spread $\sigma_\tau \to \infty$ and a channel temporal support of length N covered by the cyclic prefix).

The propagation from each interferer to BS_0 is modelled similarly to the user SS_0. It follows that the ith interferer spatial covariance (averaged with respect to the fast fading) is

$$\mathbf{Q}_I = \sum_{i=1}^{N_I} P_i \sum_{r=1}^{N_R} \rho_{\rm a}(\theta_r, \theta_i), \mathbf{a}(\theta_{i,r}) \mathbf{a}^{\rm H}(\theta_{i,r}). \quad (8)$$

depending on the DOAs $\{\theta_{i,r}\}_{r=1}^{N_R}$, the normalized power-angle-profile $\rho_{\rm a}(\theta, \theta_i)$ and the mean power P_i of the ith user, for $i = 1, \ldots, N_I$. Shadowing effects are not considered.

III. Performance analysis

In this section, the performance of the IEEE 802.16 OFDM-SIMO system is assessed in terms of average (with respect to fading) bit error probability $P_b = \Pr(b_k \neq b_k)$ at the output of the decoder applied to the spatially filtered signal (2). This performance is expected to depend on the statistics of the SINR variates $\boldsymbol{\gamma} = [\gamma_1, \ldots, \gamma_K]$, as defined in (3).

The union bound approximation for the bit error probability conditioned to the SINR set $\boldsymbol{\gamma}$ can be written as [8]

$$P_b(\boldsymbol{\gamma}) \leq \sum_{d \geq d_{\rm free}} \sum_{c \in \mathcal{E}(d)} \beta(c) P_d(\boldsymbol{\gamma}, c) \quad (9)$$

where $d_{\rm free}$ is the free Hamming distance of the code, $\mathcal{E}(d)$ is the set of all paths c having Hamming distance d from the all-zero path, $\beta(c)$ is the corresponding input weight, while $P_d(\boldsymbol{\gamma}, c)$ is the probability that the decoder chooses the path c when the all-zero codeword is transmitted (pairwise error probability, PEP). The PEP can be written as

$$P_d(\boldsymbol{\gamma}, c) = Q\left(\sqrt{2\gamma_{\rm eff}(\boldsymbol{\gamma}, c)}\right), \quad (10)$$

$\gamma_{\rm eff}(\boldsymbol{\gamma}, c)$ being the SINR at the decision variable (the *effective* SINR) for the codeword c at distance d. The effective SINR is the sum of the d SINR values $\boldsymbol{\gamma}_c = [\gamma_{f_{c,1}}, \ldots, \gamma_{f_{c,d}}]^{\rm T}$ observed over the subcarriers $\mathcal{F}_c = \{f_{c,1}, \ldots, f_{c,d}\}$ associated (by the interleaver) to the d non-zero coded bits in c:

$$\gamma_{\rm eff}(\boldsymbol{\gamma}, c) = \sum_{k \in \mathcal{F}_c} \gamma_k = \sum_{k \in \mathcal{F}_c} \left\| \tilde{\mathbf{h}}_k \right\|^2. \quad (11)$$

A further approximation of the bit error probability (9) can be obtained by upper bounding each PEP by the probability of the codeword $c_{\rm w}$ associated to the worst configuration (depending on the interleaver) of d error bits: $P_d(c) \leq P_d(c_{\rm w})$. The worst error configuration, for a given distance d, needs to be evaluated for the specific code and interlever, as done by simulations in Sec. III for the standard [1][2]. It follows that:

$$P_b(\boldsymbol{\gamma}) \leq \sum_{d \geq d_{\rm free}} \beta_d P_d(c_{\rm w}) = \sum_{d \geq d_{\rm free}} \beta_d Q\left(\sqrt{2\gamma_{\rm eff}(\boldsymbol{\gamma}, c_{\rm w})}\right) \quad (12)$$

with $\beta_d = \sum_{c \in \mathcal{E}(d)} \beta(c)$. For large SINR, the above union bound can be reasonably truncated to the minimum distance $d_{\rm free}$ term (or to the first $n > 1$ minimum distances terms, as it will be done in the following section using $n = 2$). The average bit-error probability can finally be obtained as

$$P_b = \mathrm{E}_\gamma\left[P_b(\boldsymbol{\gamma})\right] = \sum_{d \geq d_{\rm free}} \beta_d \int P_d(c_{\rm w}) p_d(\gamma_{\rm eff}) d\gamma_{\rm eff}, \quad (13)$$

where $p_d(\gamma_{\rm eff})$ is the probability density function (pdf) of the effective SINR $\gamma_{\rm eff}(\boldsymbol{\gamma}, c_{\rm w})$ for the codeword c_w at distance d.

We recall from (11) that the effective SINR $\gamma_{\rm eff}(\boldsymbol{\gamma}, c)$, associated to a generic codeword c of distance d, is the sum of the square magnitudes of Md zero-mean complex Gaussian random variables, i.e. all the channel gains associated to the positions of the errors in c, here gathered in the space-frequency vector $\tilde{\mathbf{h}}_c = [\tilde{\mathbf{h}}_{f_{c,1}}^{\rm T}, \ldots, \tilde{\mathbf{h}}_{f_{c,d}}^{\rm T}]^{\rm T}$. Thereby, the pdf $p_d(\gamma_{\rm eff})$ of this sum (for $c = c_w$) depends on the correlation among the Md channel gains, that is specified by the $Md \times Md$ correlation matrix $\mathbf{R}_c = \mathrm{E}[\tilde{\mathbf{h}}_c \cdot \tilde{\mathbf{h}}_c^{\rm H}]$. From (4), it is:

$$\mathbf{R}_c = P_0 \sum_{r=1}^{N_R} \rho(\tau_r, \theta_r)[\mathbf{g}_c(\tau_r)\mathbf{g}_c^{\rm H}(\tau_r)]^* \otimes [\tilde{\mathbf{a}}(\theta_r)\tilde{\mathbf{a}}^{\rm H}(\theta_r)]. \quad (14)$$

Here $\otimes$ denotes the Kronecker product, $\mathbf{g}_c(\tau_r)$ is the vector obtained by sampling $\mathbf{g}(\tau_r)$ at the subcarriers $\mathcal{F}_c$, while $\tilde{\mathbf{a}}(\boldsymbol{\theta}_r) = \mathbf{Q}^{-\rm H/2}\mathbf{a}(\boldsymbol{\theta}_r)$ is the spatially weighted steering vector. It is understood that the correlation degree depends on the angular/delay spread of the multipath channel (i.e., on τ_r and θ_r), compared to the spatial/temporal resolution of the system, and on the interleaving pattern (the more the error bits are spread away in the frequency domain, the lower is the correlation and the higher is the diversity).

Now, let $\mathbf{U}$ and $\boldsymbol{\lambda} = [\lambda_1 \cdots \lambda_{Md}]^{\rm T}$ be, respectively, the eigenvectors and the eigenvalues of $\mathbf{R}_c$, the effective SINR can be rewritten as $\gamma_{\rm eff}(\boldsymbol{\gamma}, c) = ||\mathbf{b}||^2$ with $\mathbf{b} = \mathbf{U}^{\rm H}\tilde{\mathbf{h}}_c$. This new formulation of the SINR is the sum of the square magnitudes

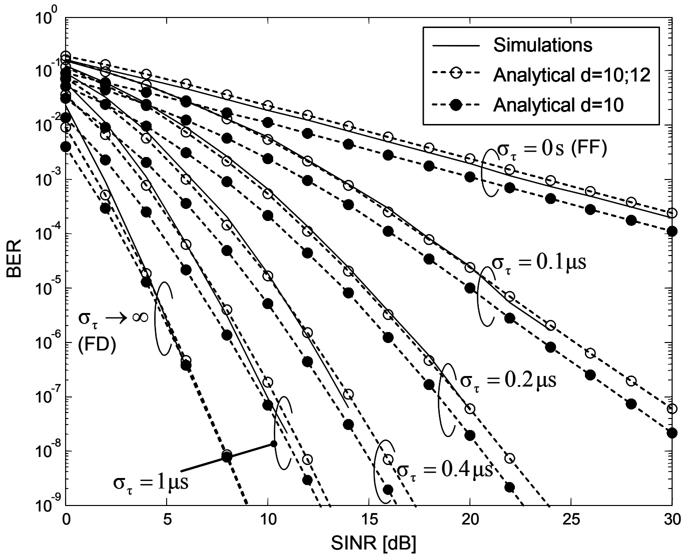

Figure 2: BER vs. SINR for a single-antenna receiver.

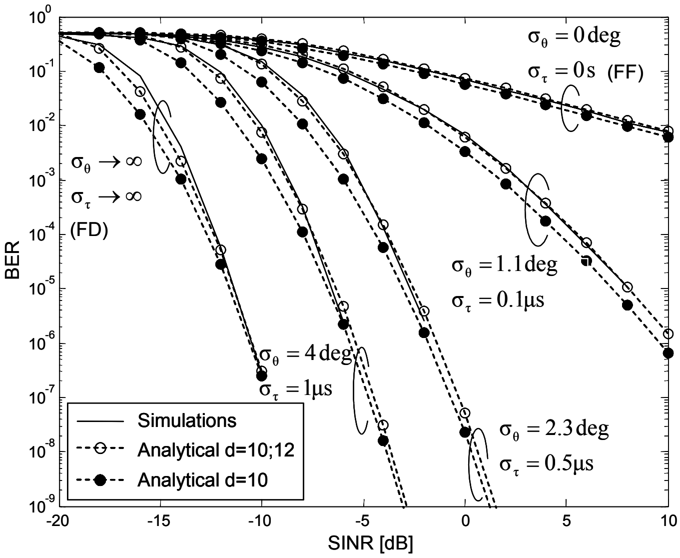

Figure 3: BER vs. SINR for a four-antenna receiver.

of Md zero-mean *independent* complex Gaussian random variables, i.e. the square magnitudes of the entries of the vector $\mathbf{b}$. As proved in [9] (p. 802), the pdf of this sum can be written as:

$$p_d(\gamma_{\text{eff}}) = \sum \frac{A_i}{\lambda_i} \exp\left(-\gamma_{\text{eff}}/\lambda_i\right), \tag{15}$$

where $A_i = 1/\Pi_{k=1,k\neq i}^{Md_{\text{free}}}(1-\lambda_k/\lambda_i)$. This latter result together with (13) allows to derive a tight bound for the average BER, as it will be shown in the following section.

Remark. The eigenvalue decomposition of the matrix $\mathbf{R}_c$ simplifies in multipath scenarios where the following Kronecker structure holds: $\mathbf{R}_c = \mathbf{R}_{\text{f}} \otimes \mathbf{R}_{\text{s}}$, being $\mathbf{R}_{\text{f}}$ the $d \times d$ correlation over the frequency and $\mathbf{R}_{\text{s}}$ the $M \times M$ correlation over the space. In such a scenario, the eigenvalues of $\mathbf{R}_c$ equal the Kronecker product of the eigenvalues of $\mathbf{R}_{\text{f}}$ and $\mathbf{R}_{\text{s}}$: $\boldsymbol{\lambda} = \boldsymbol{\lambda}_{\text{f}} \otimes \boldsymbol{\lambda}_{\text{s}}$. An example of such a Kronecker structure, adopted in the following section for performance validation, is a multipath pattern of $N_R = N_c N_m$ paths, grouped into N_c clusters of N_m multipath components each. All multipath components in the cluster have the same DOA but different TOAs: for the pth cluster, $p = 1, \ldots, N_c$, the DOA is $\theta_p = (p - (N_c + 1)/2)\Delta\theta + \theta_0$, while the W TOAs are $\tau_m = (m-1)T$ with $m = 1, \ldots, N_m$. The Kronecker structure of the space-frequency correlation matrix comes from the fact that all clusters have the same delay pattern, so it is:

$$\begin{aligned} \mathbf{R}_{\text{f}} &= \sqrt{P_0} \cdot \mathbf{F}\, \text{diag}\left(\rho_{\text{d}}(\tau_1), \ldots, \rho_{\text{d}}(\tau_{N_m})\right) \mathbf{F}^{\text{H}} \qquad (16) \\ \mathbf{R}_{\text{s}} &= \sqrt{P_0} \cdot \tilde{\mathbf{A}}\, \text{diag}\left(\rho_{\text{a}}(\theta_1, \theta_0), \ldots, \rho_{\text{a}}(\theta_{N_c}, \theta_0)\right) \tilde{\mathbf{A}}^{\text{H}} \end{aligned}$$

with $\mathbf{F}$ denoting the the $K \times W$ DFT matrix having $F_{i,m} = \exp(-j2\pi k_i m/N)$ as element (i, m) with $k_i \in \mathcal{K}$, and $\tilde{\mathbf{A}} = [\tilde{\mathbf{a}}(\theta_1) \cdots \tilde{\mathbf{a}}(\theta_{N_c})]$.

IV. Numerical results

In this section we validate the performance analysis of Sec. II by simulating a IEEE 802.16-2004 multicell scenario as the one exemplified in Fig. 1 with cell size $L = 600$m. The analytical performance is evaluated using the union bound (12) truncated to the error events at either the free distance $d = 10$, or at the two first minimum distances $d = 10$ and $d = 12$. We recall that, for each Hamming distance d, the bound (12) accounts only for the path c_w associated to the worst configuration of d error bits. The worst path c_w is independent of the delay-angle structure of the channel and it can be easily recognized as the error configuration that achieves the minimum diversity degree at the output of the periodic bit interleaver. This error configuration has been derived by numerical simulations for the specific CC and the interleaver prescribed by the standard. The performance is evaluated in the sequel as a function of the single-antenna SINR defined as

$$\text{SINR} = \frac{P_0}{\sigma_n^2 + \sum_i P_i} = \left(\frac{1}{\text{SNR}} + \frac{1}{\text{SIR}}\right)^{-1} \tag{17}$$

where $\text{SNR} = P_0/\sigma_n^2$ denotes the signal-to-noise ratio, while $\text{SIR} = P_0/\sum_{i=1}^{N_I} P_i$ is the signal-to-interference ratio. All SSs are assumed to transmit at the same power level. According to the path-loss law, the SIR depends on the ratios between the distances SS_i-BS_0 (ℓ_i) and SS_0-BS_0 (ℓ_o), for $i = 1, \ldots, N_I$, and to the path-loss exponent v: $\text{SIR} = 1/\sum_{i=1}^{N_I}(\ell_0/\ell_i)^v$. SS_0 is assumed to transmit from the main DOA $\theta_0 = 5\,\text{deg}$, while the N_I interferers are placed at the center of their cells so that $\theta_1 = -46.1\,\text{deg}, \theta_2 = 0\,\text{deg}$ and $\theta_3 = 46.1\,\text{deg}$ (see Fig. 1). Channels are simulated according to the model in Sec. I-C, with space-frequency correlation structured as at the end of Sec. II for $N_c = 35$, $\Delta\theta = 3.4$deg and temporal support equal to the cyclic prefix length $N_m = N_{cp} = 64$ (see Table 1).

We first consider a single-antenna ($M = 1$) link, with channel having exponential power delay profile (6) and delay spread $\sigma_\tau \in \{0.1; 0.2; 0.4; 1\}\mu$s. The two extreme cases of frequency selectivity $\sigma_\tau = 0$ (FF) and $\sigma_\tau \to \infty$ (FD) are also taken into account to get lower/upper performance bounds. Notice that,

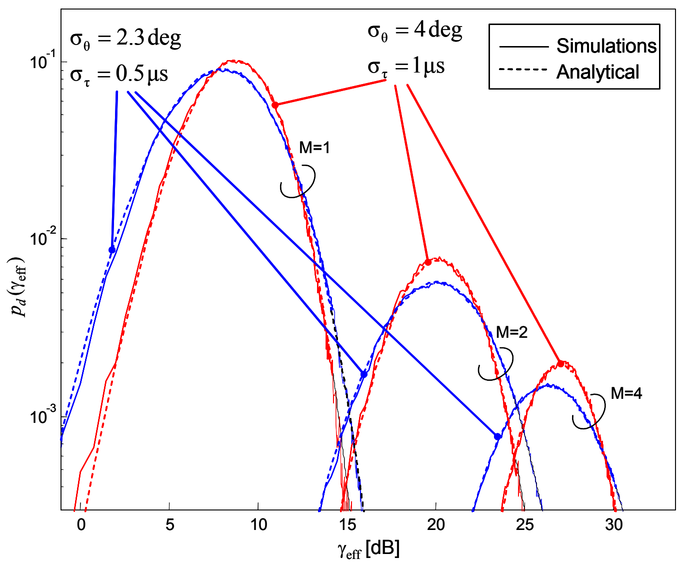

Figure 4: Pdf of the effective SINR for $d = 10$.

since the interference in this paper is assumed to be temporally-uncorrelated spatially-correlated Gaussian, for a single antenna receiver the overall noise-plus-interference signal $\mathbf{n}_k$ reduces to AWGN. Fig. 2 compares the simulated and the analytical BER vs. the average SINR for this first propagation scenario. We notice that the system performance improves when increasing the channel delay spread σ_τ, as bit-interleaved code modulation achieves large diversity gain over frequency selective channels. As expected, the worst and the best performances are obtained in the two extreme cases of frequency diversity: the error rate scales asymptotically as $1/\text{SINR}^{d_{\text{free}}}$ for the maximum diversity channel (FD) and as 1/SINR in the frequency-flat case (FF). It can be easily seen that the analytical BER derivation permits an accurate fitting of the simulation results over the whole range of average SINR and delay spread.

We now consider a ULA of $M = 4$ antennas at the base station BS_0, with inter-element spacing $\Delta = 1.4\lambda$ (λ is the carrier wavelength) chosen according to the optimum deployment in [7]. The average SNR is here set to 20 dB. The delay-angle spreads for the user SS_0 are $\sigma_\tau \in \{0.1; 0.5; 1\}\,\mu$s and $\sigma_\theta \in \{1.1; 2.3; 4\}\,\text{deg}$, while the interference angular spread is fixed to $\sigma_\theta = 4\,\text{deg}$. The single path case (for $\sigma_\theta = 0$deg and $\sigma_\tau = 0$s) and the uniform PDAP case (for $\sigma_\theta \to +\infty$ and $\sigma_\tau \to +\infty$) are considered as well. Fig. 3 shows the average BER vs. the SINR for the different space-time dispersive channel models. As expected, the minimum probability of error is obtained in rich scattering propagation environments characterized by large angle-delay spread. In this scenario, BS_0 receives the desired signal from multiple paths so that the space-frequency receiver can achieve a large diversity gain and enhance the transmission reliability. On the other hand, when the physical channel exhibits a strong correlation, the spatial filter is devoted to mitigate the out-of-cell interference impairments; in this scenario the multiantenna system achieves limited diversity and the transmission shows reduced robustness against fading deeps. In all cases, the proposed analytical framework is shown to provide an efficient performance assessment.

For the free Hamming distance, in Fig. 4 the pdf of the effective SINR is evaluated from numerical results and compared to the analytical expression (15), for the same simulation setting as in Fig. 3 and SINR= 0 dB. The number of antennas here takes values $M \in \{1; 2; 4\}$, while the angle-delay spread for the SS_0 channel is either $(\sigma_\theta, \sigma_\tau) = (2.3\,\text{deg}, 0.5\mu\text{s})$ or $(\sigma_\theta, \sigma_\tau) = (4\,\text{deg}, 1\mu\text{s})$. The figure shows that the analytical distribution based on the eigenvalue decomposition of the space-frequency covariance matrix permits an efficient fitting of the distribution of the SINR at the decision variable.

V. Conclusions

In this paper an accurate framework has been proposed to analytically assess the performance of a multiantenna multicell WiMax systems. The analysis encompasses heterogeneous propagation scenarios according to different degrees of spatial and temporal diversity. This study, validated by numerical results, shows that the communication system is very effective in rich scattering environments, whereas the performance deteriorates considerably for strongly correlated channels with moderate angle-delay spread.

References

[1] IEEE Std 802.16™-2004, "802.16™ IEEE standard for local and metropolitan area networks Part 16: Air interface for fixed broadband wireless access systems," Oct. 2004.

[2] IEEE P802.16-2004/Cor1/D5 (Draft Corrigendum to IEEE Std 802.16-2004), "Corrigendum to IEEE standard for local and metropolitan area networks - Part 16: Air interface for fixed broadband wireless access systems," Sept. 2005.

[3] S. Nanda, K. M. Rege, "Frame error rates of convolutional codes on fading channels and the concept of effective E_b/N_0," *IEEE Trans. Veh. Technol.*, Vol. 47, No. 4, pp 1245-1250, Nov. 1998.

[4] K. Witrisal, Yong-Ho Kim, R. Prasad, "A novel approach for performance evaluation of OFDM with error correction coding and interleaving," *Proc. IEEE Veh. Technol. Conf. (VTC'99-Fall)*, Vol. 1, pp. 294-299, Sept. 1999.

[5] M.S. Alouini, A. Abdi, M. Kaveh, "Sum of gamma variates and performance of wireless communication systems over Nakagami-fading channels," *IEEE Trans. Veh. Technol.*, Vol. 50, No. 6, pp. 1471-1480, Nov. 2001.

[6] R. Bosisio and U. Spagnolini, "Collision model for the bit error rate analysis of multicell multiantenna OFDMA systems," *Proc. IEEE Int. Conf. Commun. (ICC'07)*, June 2007.

[7] M. Nicoli, L. Sampietro, C. Santacesaria, S. Savazzi, O. Simeone, U. Spagnolini, "Throughput optimization for non-uniform linear antenna arrays in multicell WiMAX systems," *Proc. IEEE Workshop on Smart Antennas (WSA'06)*, Mar. 2006.

[8] M.K. Simon, M.S. Alouini, *Digital Communication over Fading Channels: an Unified Approach to Performance Analysis*. Wiley, 2000.

[9] J.G. Proakis, *Digital Communications*, 4th ed. McGraw Hill, 2001.

[10] H. L. Van Trees, *Optimum Array Processing*. Wiley, 2002.